# ON THE EVALUATION OF DILATOMETER EXPERIMENTS

**Dietmar Hömberg**[1], **Nataliya Togobytska**[1], **Masahiro Yamamoto**[2]

[1] Weierstrass Institute for Applied Analysis and Stochastics
Mohrenstr. 39, 10117 Berlin, Germany
E-Mail: hoemberg@wias-berlin.de, togobytska@wias-berlin.de

[2] Department of Mathematical Sciences, The University of Tokyo
3–8–1 Komaba Meguro, Tokyo 153-8914, Japan
E-Mail: myama@ms.u-tokyo.ac.jp

Abstract. The goal of this paper is a mathematical investigation of dilatometer experiments. These are used to detect the kinetics of solid-solid phase transitions in steel upon cooling from the high temperature phase. Usually, the data are only used for measuring the start and end temperature of the phase transition. In the case of several coexisting product phases, expensive microscopic investigations have to be performed to obtain the resulting fractions of the different phases. In contrast, it is shown in this paper that in the case of at most two product phases the complete phase transition kinetics including the final phase fractions are uniquely determined by the dilatometer data. Numerical results confirm the theoretical result.

2000 *Mathematics Subject Classification.* 35R30, 74F05, 74N99.

*Key words and phrases.* Dilatometer, phase transitions, inverse problem.

D. Hömberg was partially supported by the DFG Research Center Matheon "Mathematics for key technologies". N. Togobytska was supported by the DFG SPP 1204 "Algorithms for fast, material specific process-chain design and -analysis in metal forming". M. Yamamoto was partly supported by Grant 15340027 from the Japan Society for the Promotion of Science and Grant 17654019 from the Ministry of Education, Cultures, Sports and Technology.

## 1. Introduction

The dilatometer is an instrument for magnifying and measuring expansion and contraction of a solid during heating and subsequent cooling. It is often used in the determination of phase transitions occurring with the change of temperature in the heat-treatment of steels. Figure 1 depicts a typical measurement setup of dilatometers. The steel specimen is contained in a heating device, usually induction heating.Through a rod on its right-hand side, length changes $\lambda(t)$ due to compression or expansion are measured as a function of time $t$. In addition the temperature $\tau(t)$ is measured. In Section 2, we describe the governing equations (2.5) - (2.9) for displacement $u$ and temperature $\theta$ and then we have $\lambda(t) = u(1,t)$ and $\tau(t) = \theta(x_0,t)$, where $x_0$ is an observation point in a domain under consideration.

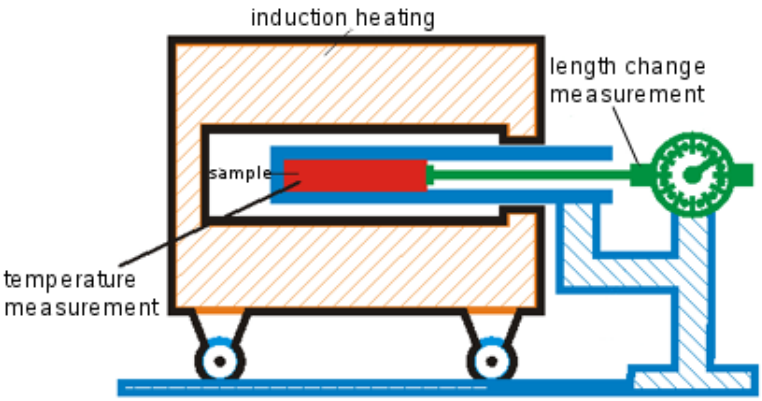


Figure 1. Sketch of the dilatometer experiment.

Usually, the results are documented in a dilatometer curve, where length change is plotted versus temperature, parameterized by the time $t$. A typical dilatometer curve for the cooling of a specimen made of eutectoid carbon steel is shown in Figure 2.

The part of the curve to the right of point $A$ shows the normal contraction of the specimen during slow cooling for a steel in the austenitic phase. At point $A$ a phase transition (from austenite to pearlite) starts and it ends at point $B$. Then again a period with linear contraction prevails followed by another phase transition (austenite to martensite) between $C$ and $D$, and finally another linear contraction period. Therefore the main information drawn from such a dilatometer experiment usually are the start $(T_A, T_C)$ and end $(T_B, T_D)$ temperatures of the occurring phase transitions. Moreover, one knows that above $T_A$ the state is purely austenitic. Between $T_B$ and $T_C$ there is a constant mixture of austenite and pearlite and below $T_D$ we have a mixture of the product phases pearlite and

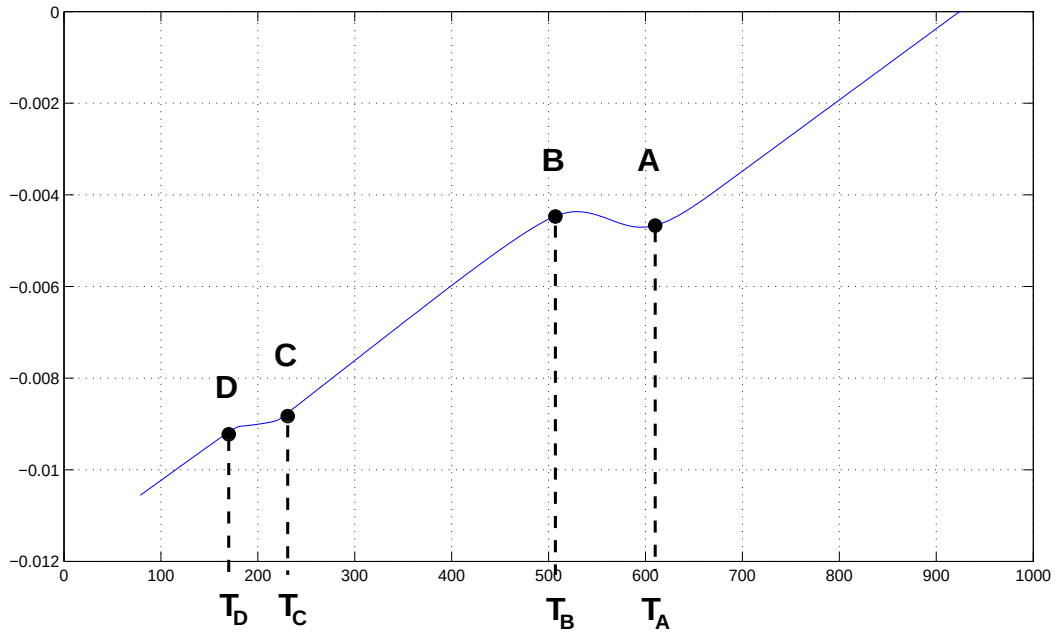


FIGURE 2. Dilatometer curve for steel C 1080 exhibiting 2 phase transitions.

martensite. Usually, these data are used to derive so-called Continuous-Cooling-Transformation (CCT) diagrams, which illustrate the beginning and end of a phase transition during continuous cooling.

This approach has two drawbacks. First of all, depending on the curvature of the respective dilatometer curve, it might become rather difficult and erroneous to fix transformation points $A, \ldots, D$. Secondly, in the case of two phase transitions as in Figure 2, the actual phase fractions of the different product phases cannot be drawn directly from the dilatometer curve. Therefore, usually costly polished micrograph sections have to be made and investigated under the microscope. The precision of the predicted phase fractions then highly depends on the experience of the respective experimenter.

From a mathematical point of view, deriving just the four critical temperatures is like a waste of information. Indeed it is the goal of this paper to prove that one can uniquely identify the evolution of two product phases $y(t)$ and $z(t)$ from the measurements $\tau(t)$ and $\lambda(t)$. We refer for example, to [5] as a source book concerning similar inverse problems, and see also [3] concerning a similar treatment of inverse problems.

The outline of the paper is as follows. In the next section we will give a precise problem formulation. In Section 3 we prove the identifiabilty result. The last

section is devoted to numerical examples for the solution of the identification problem.

## 2. Problem formulation

The standard shape for dilatometer specimen is a cylinder. Since the diameter is small compared to its length, we will neglect radial variations of the physical quantities and just consider variations along the symmetry axis. For convenience, we define

$$\Omega = (0, 1),$$

and assume small deformations which will allow us to write down the equations in the undeformed domain.

We assume that at most two phase transitions may occur during cooling, with phase fractions $y(t)$ and $z(t)$, respectively, depending only on time $t$ but not on space. In addition, they satisfy

(2.1)

$$y(0) = z(0) = 0, \quad 0 \le y(t), \qquad 0 \le z(t), \qquad y(t)+z(t) \le 1, \qquad \text{for all } t \in [0, T],$$

The simplest model to describe a thermal expansion as indicated in Figure 2 is assuming a mixture ansatz for the thermal strain

$$\varepsilon^{th} = y\varepsilon_1^{th} + z\varepsilon_2^{th} + (1 - y - z)\varepsilon_0^{th}, \tag{2.2}$$

where the thermal strain in each phase is given by the linear model

$$\varepsilon_i^{th} = \delta_i(\theta - \theta_{ref}^i). \tag{2.3}$$

Here the constants $\delta_i > 0$ is the thermal expansion coefficient and $\theta_{ref}^i$ the reference temperature. For convenience we define

$$\alpha_1 = \delta_1 - \delta_0, \quad \alpha_2 = \delta_2 - \delta_0, \quad \beta_1 = \delta_1\theta_{ref}^1 - \delta_0\theta_{ref}^0, \quad \beta_2 = \delta_2\theta_{ref}^2 - \delta_0\theta_{ref}^0.$$

Setting $w = (y, z)$ and

$$\delta(w) = \alpha_1 y + \alpha_2 z + \delta_0, \quad \eta(w) = \beta_1 y + \beta_2 z + \delta_0\theta_{ref}^0, \tag{2.4}$$

we obtain for the overall thermal strain

$$\varepsilon^{th} = \delta(w)\theta - \eta(w).$$

Moreover by (2.1), we see that

$$\delta(w(t)) \ge \min\{\delta_0, \delta_1, \delta_2\} > 0.$$

Assuming furthermore an additive partitioning of the overall strain into a thermal and an elastic one, i.e. $\varepsilon = \varepsilon^{el} + \varepsilon^{th}$ we obtain the following quasi- static linearized

thermo-elasticity system:

$$\big(u_x - \delta(w)\theta + \eta(w)\big)_x = 0, \quad \text{in } \Omega \times (0,T) \tag{2.5}$$

$$\rho c\theta_t - k\theta_{xx} + \Lambda\delta(w)u_{xt} - \rho L_1 y' - \rho L_2 z' = \gamma(\theta^e - \theta), \quad \text{in } \Omega \times (0,T) \tag{2.6}$$

$$u(0,t) = 0, \quad u_x(1,t) - \delta(w)\theta(1,t) + \eta(w) = 0, \quad \text{in } (0,T) \tag{2.7}$$

$$\theta_x(0,t) = \theta_x(1,t) = 0, \quad \text{in } (0,T) \tag{2.8}$$

$$\theta(\cdot,0) = \theta_0, \quad \text{in } \Omega. \tag{2.9}$$

Here, we set $y' = \frac{dy}{dt}$, $\rho$ is the density, $c$ the heat capacity, and $k$ is the thermal conductivity, $L_1$ and $L_2$ are the latent heats of the phase transitions. The constant $\Lambda = 2\Lambda_1 + \Lambda_2$ is the bulk modulus with the Lamé coefficients $\Lambda_1, \Lambda_2$. Since the cooling happens all around the specimen, we have chosen a distributed Newton type of cooling law, with the heat exchange coefficient $\gamma$, and $\theta^e$ is the temperature of the coolant. In view of Hooke's law, the stress $\sigma$ is given by

$$\sigma = u_x - \delta(w)\theta + \eta(w),$$

hence, the second boundary condition for $u$ just states that the specimen is stress-free at $x = 1$. $L_1$ and $L_2$ are the latent heats of the phase transitions. All other constants have been normalized to one without loss of generality. We make the following assumptions

**(A1):** $L_1, L_2, \delta_1, \delta_2, \delta_3, \gamma > 0$
**(A2):** $\theta_0, \theta^e \in C[0,T]$ satisfying $\theta_0(x) > \theta^e(x) > 0$ for all $x \in [0,T]$,
**(A3):** $y, z \in C^1[0,T]$ such that $y', z' \geq 0$ for all $t \in [0,T]$ and there exists a constant $M > 0$ such that $\|y\|_{C^1[0,T]}, \|z\|_{C^1[0,T]} \leq M$, and (2.1) is satisfied.
**(A4):** $y'(t) = z'(t) = 0$ for $\theta \leq \theta^e$.

(A2) reflects the fact that we consider a cooling experiment, i.e., we start with a hot specimen, while (A4) rephrases that there are no phase transitions below temperature $\theta^e$. For the direct problem, we have the following

**Lemma 2.1.** *Assume (A1)–(A3), then* (2.5)–(2.9) *admits a unique classical solution* $(u,\theta)$. *Moreover, it satisfies* $\theta(x,t) \geq \theta^e$ *in* $\Omega \times (0,T)$, *if also (A4) holds.*

**Remark 2.1.** *As seen in Figure 2 the the phase transitions are finished when temperature* $T_D$ *is reached. Hence it is natural to assume that* $y'(t) = z'(t) = 0$ *for* $\theta \leq \theta^e$ *if the latter is less than* $T_D$.

**Proof:**
Showing the existence of a unique solution to the state system is a standard task which we omit here. Instead, we refer to [4]. To show the non-negativity of $\theta$, we first note that (2.5) implies the existence of a function $\mu$ depending only on time, such that

$$u_x - \delta(w)\theta + \eta(w) = \mu(t), \quad \text{for all } (x,t) \in \bar{\Omega} \times (0,T).$$

Regarding (2.7), we see that $\mu \equiv 0$, hence we have

$$u_x = \delta(w)\theta - \eta(w), \quad \text{for all } (x,t) \in \bar{\Omega} \times (0,T). \tag{2.10}$$

Differentiating (2.10) formally with respect to $t$, we can infer

$$u_{xt} = (\alpha_1 y' + \alpha_2 z')\theta + \delta(w)\theta_t - \beta_1 y' - \beta_2 z'. \tag{2.11}$$

Inserting this into (2.6), we obtain

$$(1+\nu\delta(w)^2)\theta_t - \kappa\theta_{xx} + \nu\delta(w)(\alpha_1 y' + \alpha_2 z')\theta = \hat{L}_1(w)y' + \hat{L}_2(w)z' + \hat{\gamma}(\theta^e - \theta), \tag{2.12}$$

with

$$\hat{L}_1(w) = \frac{L_1}{c} + \nu\delta(w)\beta_1, \quad \hat{L}_2(w) = \frac{L_2}{c} + \nu\delta(w)\beta_2 \tag{2.13}$$

and

$$\kappa = \frac{k}{\rho c}, \quad \nu = \frac{\Lambda}{\rho c}, \quad \hat{\gamma} = \frac{\gamma}{\rho c}.$$

To prove the lower bound for $\theta$, we test (2.12) with $\theta_- := \min\{\theta - \theta^e, 0\}$, integrate by parts, and use the identity $\theta = \theta^e + \theta_- + \theta_+$ to obtain

$$\begin{aligned}
&\int_0^t \int_\Omega (1+\nu\delta(w)^2)\frac{1}{2}\frac{\partial}{\partial s}\theta_-^2 dxdt + \kappa \int_0^t \int_\Omega \theta_x \theta_{-,x} dxdt + \int_0^t \int_\Omega \nu\delta(w)(\alpha_1 y' + \alpha_2 z')\theta\theta_- dxdt \\
&\quad = \frac{1}{2}\int_\Omega (1+\nu\delta(w)^2)\theta_-^2(t)dxdt + \kappa \int_0^t \int_\Omega \theta_{-,x}^2 dxdt \\
&\quad = \int_0^t \int_\Omega (\hat{L}_1(w)y' + \hat{L}_2(w)z')\theta_- dxdt + \hat{\gamma}\int_0^t \int_\Omega (\theta^e - \theta)\theta_- dxdt \\
&\quad \leq 0.
\end{aligned}$$

The latter inequality holds in view of (A1)–(A4). From this we can infer $\theta_-(x,t) = 0$.

## 3. A stability result for the inverse problem

In this section we study the inverse problem of reconstructing the phase fractions of at most two product phases from measured data $u(1,t)$ and $\theta(x_0,t)$ for $t \in [0,T]$ at some point $x_0 \in (0,1)$. For given $w(t) = (y(t), z(t))$ and $\lambda(t)$, we set

$$\begin{aligned}
\mathcal{L}_1(\lambda(t), w(t)) &= \frac{L_1}{c} + \frac{\lambda(t) + \eta(w(t))}{\delta^2(w(t))}\alpha_1 - \frac{\beta_1}{\delta(w(t))}, \\
\mathcal{L}_2(\lambda(t), w(t)) &= \frac{L_2}{c} + \frac{\lambda(t) + \eta(w(t))}{\delta^2(w(t))}\alpha_2 - \frac{\beta_2}{\delta(w(t))},
\end{aligned}$$

and we recall that $\hat{L}_1(w)$ and $\hat{L}_2(w)$ are defined by (2.13).

For our inverse problem, we have to enforce the additional assumption:

**(A5):** For $w(t), \theta, u$ satisfying (2.5) - (2.9), there holds,

$$\mathcal{L}_1(u(1,t),w(t))(\hat{L}_2(w(t)) - \nu\delta(w(t))\alpha_2\theta(x_0,t)) \\ -\mathcal{L}_2(u(1,t),w(t))(\hat{L}_1(w(t)) - \nu\delta(w(t))\alpha_1\theta(x_0,t)) \neq 0, \quad 0 \leq t \leq T.$$

**Remark 3.1.** *In the next section we will show that assumption (A4) indeed is satisfied for realistic physical data.*

Our main result is the following global stability estimate:

**Theorem 3.1.** *Let $(y_i, z_i)$, $i = 1, 2$ be two sets of phase fractions such that (A1)–(A4) are satisfied and let $(u_i, \theta_i)$, $i = 1, 2$, be the corresponding solutions to* (2.5)–(2.9).

*Then there exists a constant $C > 0$ such that*

$$\|y_1 - y_2\|_{C^1[0,T]} + \|z_1 - z_2\|_{C^1[0,T]} \\ \leq C(\|(u_1 - u_2)(1,\cdot)\|_{C^1[0,T]} + \|(\theta_1 - \theta_2)(x_0,\cdot)\|_{C^1[0,T]}).$$

**Proof:**

By (2.10) we have

$$\int_0^x \partial_x u_j(\xi,t)d\xi = \int_0^x \delta(w_j(t))\theta_j(\xi,t)d\xi - \int_0^x \eta(w_j(t))d\xi,$$

and by (2.7), we obtain

$$u_j(x,t) = \delta(w_j(t)) \int_0^x \theta_j(\xi,t)d\xi - x\eta(w_j(t)), \quad t > 0.$$

Defining

$$\lambda_j(t) \equiv u_j(1,t),$$

we obtain

$$\lambda_j(t) = \delta(w_j(t)) \int_0^1 \theta_j(\xi,t)d\xi - \eta(w_j(t)), \quad x > 0. \tag{3.1}$$

Now, we integrate (2.12) over $x \in (0,1)$, use (2.8) and (3.1):

$$(1 + \nu\delta(w_j(t))^2) \left( \frac{\lambda_j(t) + \eta(w_j(t))}{\delta(w_j(t))} \right)' + \nu(\lambda_j(t) + \eta(w_j(t)))(\alpha_1 y_j' + \alpha_2 z_j') \\ = \hat{L}_1(w_j)y_j' + \hat{L}_2(w_j)z_j' - \hat{\gamma}\frac{\lambda_j(t) + \eta(w_j(t))}{\delta(w_j(t))} + \hat{\gamma}\theta^e, \quad t > 0.$$

Rearranging terms yields

$$\mathcal{L}_1(\lambda_j(t), w_j(t))y_j'(t) + \mathcal{L}_2(\lambda_j(t), w_j(t))z_j'(t) \\ = \left(1 + \nu\delta^2(w_j(t))\right) \frac{\lambda_j'(t)}{\delta(w_j)} + \hat{\gamma}\frac{\lambda_j(t) + \eta(w_j(t))}{\delta(w_j(t))} - \hat{\gamma}\theta^e, \quad t > 0. \tag{3.2}$$

Now we define $\bar{\lambda} = \lambda_1 - \lambda_2$ and analogously $\bar{y}$ and $\bar{z}$, then we take the difference of (3.2) for $j = 1, 2$:

$$\begin{aligned}
&\mathcal{L}_1(\lambda_1, w_1)\bar{y}'(t) + \mathcal{L}_2(\lambda_1, w_1)\bar{z}'(t) \\
&\quad + \quad (\mathcal{L}_1(\lambda_1, w_1) - \mathcal{L}_1(\lambda_2, w_2))y_2' + (\mathcal{L}_2(\lambda_1, w_1) - \mathcal{L}_2(\lambda_2, w_2))z_2' \\
&\qquad = (1 + \nu\delta(w_1)^2)\frac{\lambda_1'}{\delta(w_1)} - (1 + \nu\delta(w_2)^2)\frac{\lambda_2'}{\delta(w_2)} \\
&\qquad\quad + \hat{\gamma}\left(\frac{\lambda_1 + \eta(w_1)}{\delta(w_1)} - \frac{\lambda_2 + \eta(w_2)}{\delta(w_2)}\right).
\end{aligned}$$

We can rewrite them as

$$\mathcal{L}_1(\lambda_1, w_1)\bar{y}'(t) + \mathcal{L}_2(\lambda_1, w_1)\bar{z}'(t) = K_1(\bar{\lambda}, \bar{\lambda}') + K_2(\bar{y}, \bar{z}), \quad 0 < t < T. \tag{3.3}$$

Here and henceforth, $K_i$, $\widetilde{K_i}$, $K_i^{(1)}$ are linear functions in the arguments whose coefficients are bounded in $C[0, T]$ by $M$. We set $\bar{\theta} = \theta_1 - \theta_2$.

Next, we take the difference of (2.12) for $j = 1, 2$, leading to

$$\begin{aligned}
&\left(1 + \nu\delta(w_1)^2\right)\bar{\theta}_t - \kappa\bar{\theta}_{xx} + \nu(\delta(w_1) + \delta(w_2))\partial_t\bar{\theta}_2(\alpha_1\bar{y} + \alpha_2\bar{z}) \\
&\quad + \quad \nu\delta(w_2)(\alpha_1 y_2' + \alpha_2 z_2')\bar{\theta} + \nu\delta(w_1)\theta_1(\alpha_1\bar{y}' + \alpha_2\bar{z}') \\
&\quad + \quad \nu(\alpha_1 y_2' + \alpha_2 z_2')\theta_1(\alpha_1\bar{y} + \alpha_2\bar{z}) \\
&\qquad = \hat{L}_1(w_1)\bar{y}' + \hat{L}_2(w_1)\bar{z}' + \nu(\beta_1 y_2' + \beta_2 z_2')(\alpha_1\bar{y} + \alpha_2\bar{z}) - \hat{\gamma}\bar{\theta}.
\end{aligned}$$

The latter we will rewrite it as

$$\begin{aligned}
&\left(1 + \nu\delta(w_1)^2\right)\bar{\theta}_t - \kappa\bar{\theta}_{xx} + \nu(\delta(w_2)(\alpha_1 y_2' + \alpha_2 z_2') + \hat{\gamma})\bar{\theta} \\
&\qquad = \quad (\hat{L}_1(w_1) - \nu\delta(w_1)\alpha_1\theta_1)\bar{y}' + (\hat{L}_2(w_1) - \nu\delta(w_1)\alpha_2\theta_1)\bar{z}' \\
&\qquad\qquad + K_3(\bar{y}, \bar{z}), \qquad 0 < x < 1,\, t > 0
\end{aligned} \tag{3.4}$$

and

$$\bar{\theta}(x, 0) = 0, \quad \bar{\theta}_x(0, t) = \bar{\theta}_x(1, t) = 0, \quad 0 < x < 1,\, t > 0. \tag{3.5}$$

Henceforth, by $U(t, s)$ we denote the evolution operator generated by

$$A(t) = \frac{-1}{1 + \nu\delta(w_1)^2}(\kappa\partial_x^2 - \nu\delta(w_2(t))(\alpha_1 y_2' + \alpha_2 z_2') - \hat{\gamma})(\cdot)$$

and

$$\mathcal{D}(A(t)) = \{\eta \in H^2(0, 1);\, \eta_x(0) = \eta_x(1) = 0\}$$

(e.g., Chapter 5 in Tanabe [7]).

This allows us to recast (3.4) and (3.5) as

$$\begin{aligned}
\bar{\theta}'(t) &= A(t)\bar{\theta}(t) + \frac{\hat{L}_1(w_1) - \nu\delta(w_1)\alpha_1\theta_1}{1 + \nu\delta(w_1)^2}\bar{y}' \\
&\quad + \frac{\hat{L}_2(w_1) - \nu\delta(w_1)\alpha_2\theta_1}{1 + \nu\delta(w_1)^2}\bar{z}' + \frac{K_3(\bar{y}, \bar{z})(t)}{1 + \nu\delta(w_1)^2}, \quad t > 0
\end{aligned} \tag{3.6}$$

and $\bar\theta(0)=0$. Here, we write $\bar\theta(t)=\bar\theta(\cdot,t)$. In particular, $\partial_s U(t,s)=U(t,s)A(s)$. Then we have for $0<t<T$

$$\bar\theta(t)=\int_0^t U(t,s)\frac{\hat L_1(w_1)-\nu\delta(w_1)\alpha_1\theta_1}{1+\nu\delta(w_1)^2}\bar y'(s)ds + \int_0^t U(t,s)\frac{\hat L_2(w_1)-\nu\delta(w_1)\alpha_2\theta_1}{1+\nu\delta(w_1)^2}\bar z'(s)ds+\int_0^t U(t,s)\frac{K_3(\bar y,\bar z)(s)}{1+\nu\delta(w_1)^2}ds.$$

Differentiating the both sides, we have

$$\bar\theta'(t)=\frac{\hat L_1(w_1)-\nu\delta(w_1(t))\alpha_1\theta_1(t)}{1+\nu\delta(w_1(t))^2}\bar y'(t)+\frac{\hat L_2(w_1)-\nu\delta(w_1(t))\alpha_2\theta_1(t)}{1+\nu\delta(w_1(t))^2}\bar z'(t) + \int_0^t \widetilde{K_4}(\bar y',\bar z')(s)ds+\widetilde{K_5}(\bar y,\bar z)(t)+\int_0^t\widetilde{K_6}(\bar y,\bar z)(s)ds.$$

Defining $\bar\tau=\bar\theta(x_0,.)$, we obtain

$$\frac{\hat L_1(w_1)-\nu\delta(w_1(t))\alpha_1\theta_1(x_0,t)}{1+\nu\delta(w_1(t))^2}\bar y'(t)+\frac{\hat L_2(w_1)-\nu\delta(w_1(t))\alpha_2\theta_1(x_0,t)}{1+\nu\delta(w_1(t))^2}\bar z'(t) = \bar\tau'(t)-\int_0^t K_4(\bar y',\bar z')(s)ds-K_5(\bar y,\bar z)(t)-\int_0^t K_6(\bar y,\bar z)(s)ds. \tag{3.7}$$

In view of (A4), we can solve (3.3) and (3.7) with respect to $\bar y'$ and $\bar z'$, and we obtain

$$\bar y'(t)=K_7(\bar\lambda,\bar\lambda',\bar\tau')+K_8(\bar y,\bar z) + \int_0^t (K_9(\bar y,\bar z)(s)+K_{10}(\bar y',\bar z')(s))ds,\quad 0\le t\le T.$$

Noting that $\bar y(0)=0$, we have

$$|K_8(\bar y,\bar z)(t)|,\ |K_9(\bar y,\bar z)(t)|\le C\int_0^t(|\bar y'(s)|+|\bar z'(s)|)ds.$$

Mutatis mutandis, the same reasoning holds for $\bar z(t)'$. Altogether, we obtain

$$|\bar y'(t)|+|\bar z'(t)| \le C(|\bar\lambda(t)|+|\bar\lambda'(t)|+|\bar\tau'(t)|)+C\int_0^t(|\bar y'(s)|+|\bar z'(s)|)ds,\quad 0\le t\le T.$$

The Gronwall inequality yields

$$|\bar y'(t)|+|\bar z'(t)|\le C(\|\bar\lambda\|_{C^1[0,T]}+\|\bar\tau\|_{C^1[0,T]}),\quad 0\le t\le T.$$

Thus the proof is completed.

**Remark 3.2.** *We can expect the existence of $(y, z)$ satisfying (2.5) - (2.9) and realizing given data for $u(1, \cdot)$ and $\theta(x_0, \cdot)$, but we here exploit only the stability, which is an important theoretical issue for numerical computations.*

| symbol | value | unit | symbol | value | unit |
|---|---|---|---|---|---|
| $\rho$ | 7.85 | $[g/cm^3]$ | $c$ | 0.5096 | $[J/(gK)]$ |
| $k$ | 0.5 | $[J/(s*cm*K)]$ | $\Lambda_1$ | $1.0724e+5$ | $[Pa]$ |
| $\Lambda_2$ | $6.882e+4$ | $[Pa]$ | $L_1$ | 77.0 | $[J/g]$ |
| $L_2$ | 84.0 | $[J/g]$ | $\delta_0$ | $1.55e-5$ | $[1/K]$ |
| $\delta_1$ | $1.7e-5$ | $[1/K]$ | $\delta_2$ | $1.16e-5$ | $[1/K]$ |
| $\theta^0_{ref}$ | 1473 | $K$ | $\theta^1_{ref}$ | 1234 | $K$ |
| $\theta^2_{ref}$ | 773 | $K$ | | | |

TABLE 1. Metallurgical parameters for the carbon steel C1080.

## 4. Numerical results

In this section we present some results for the numerical identification of phase fractions $y(t), z(t)$ from dilatometer curves, or more precisely, from measurements $\hat{\lambda}$ of the overall displacement $\lambda(t) = u(1, t)$, as well as measurements $\hat{\tau}(t)$ of the temperature in one point, $\tau(t) = \theta(x_0, t)$. To this end, we solve the optimal control problem

$$\min \Big\{ \omega_1 \int_0^T (u(1,t) - \hat{\lambda}(t))^2 dt + \omega_2 \int_0^T (\theta(x_0,t) - \hat{\tau}(t))^2 dt \Big\}$$

subject to the state sytem (2.5)–(2.9) and the control constraint $y, z \in U_{ad}$.

The state system is discretized using finite differences. The phase fraction functions to be determined are represented as cubic splines. Enforcing the additional conditions

$$y(0) = z(0) = y'(0) = z'(0) = y'(T) = z'(T) = 0$$

the remaining spline coefficients can be uniquely represented in terms of the values of $y, z$ in the temporal grid points $t_1, \dots, t_n$. Defining the parameter vector

$$p = (y(t_1), \dots y(t_n), z(t_1), \dots y(t_n)$$

we consider the nonlinear optimization problem

$$\min \Big\{ \omega_1 \sum_{i=1}^n (u(1,t_i,p) - \hat{\lambda}(t_i))^2 dt + \omega_2 \sum_{i=1}^n (\theta(x_0,t_i,p) - \hat{\tau}(t_i))^2 dt \Big\} \tag{4.1}$$

subject to a discretized version of the state sytem (2.5)–(2.9)

and the control constraint $p \in \widetilde{U}_{ad}$.

So far our approach has only been tested on model data for the plain carbon steel C 1080. Table 1 summarizes the metallurgical data used for the simulations. Now, we are in a position to check the validity of assumption (A4). In view of the data in Table 1, we can conclude

$$\delta_2 \leq \delta(w) \leq \delta_1.$$

Since we cool below $M_f$, we have indeed $y'(t) = z'(t) = 0$ for $\theta < \theta^e$. Hence, we have

$$\lambda(t) + \eta(w(t)) \geq |\Omega|\theta^e, \quad \delta^2(w(t))\theta(x_0, t)) \geq \delta_2^2\theta^e.$$

Inserting the data for $L_{1,2}, \alpha_{1,2}, \beta_{1,2}$, it is easily seen that the complete expression stays negative, hence we can conclude that (A4) is satisfied.

To generate the model data, we have solved the system of state equations (2.5)–(2.9) together with two rate laws for $y$ and $z$ (cf. [1], see also [2] for more general phase transitions models):

$$y' = (1 - y - z)g(\theta) \tag{4.2}$$

$$z' = 5[\hat{z} - z_2, 0]_+ \tag{4.3}$$

with

$$\hat{z} = \min\{\bar{m}, 1 - y\}$$

and $\bar{m}(\theta) = 1$, if $\theta < M_f$, $\bar{m}(\theta) = 0$, if $\theta > M_s$. In between it is defined as the linear interpolation between 0 and 1. Here, $M_{s,f}$ are the starting and finishing temperatures for the martensitic growth, which for the steel C1080 take the values

$$M_s = 500K \qquad M_f = 366K.$$

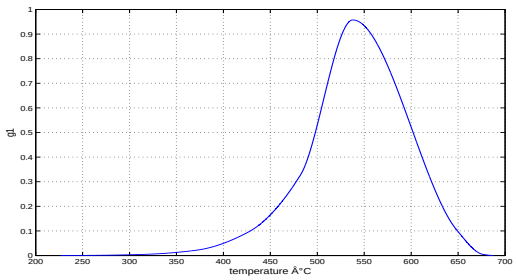


FIGURE 3. The data function $g(\theta)$ in (4.2).

As before, we denote $[x]_+ = \max\{x, 0\}$. System (4.2)–(4.3) is explained in more detail in [1]. A rough explanation is that the growth rate of pearlite, $y'$, is assumed to be proportinal to the remaining fraction of the high temperature phase and a function depending only on temperature (cf. Figure 3), while the second phase,

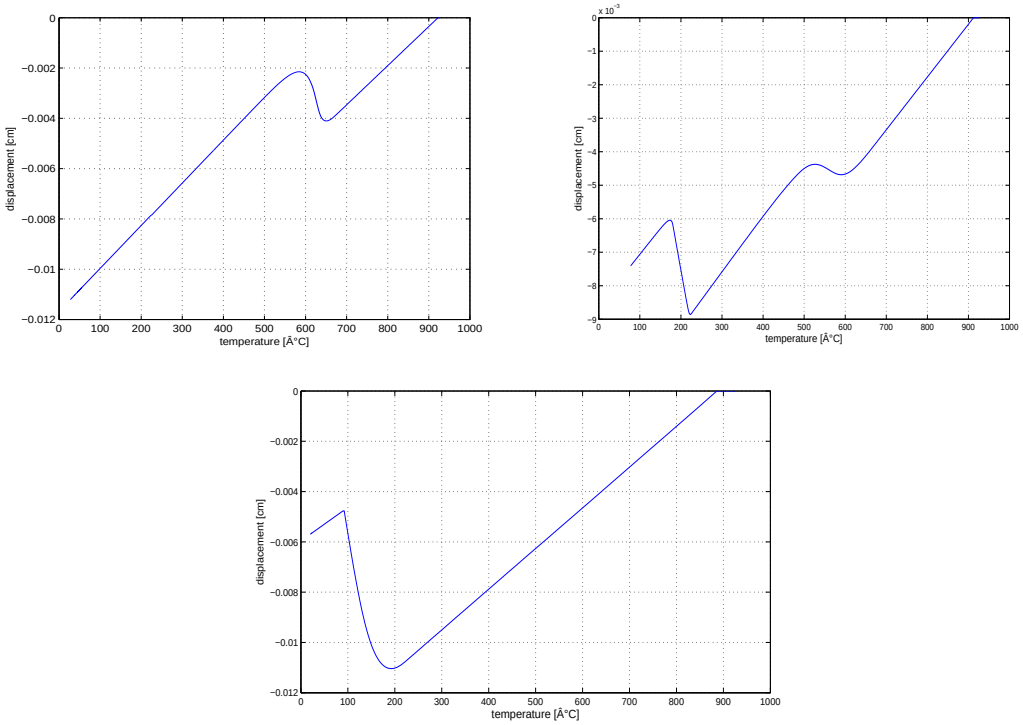


FIGURE 4. Model dilatometer curves for slow (top left), medium (top right) and fast (bottom) quenching.

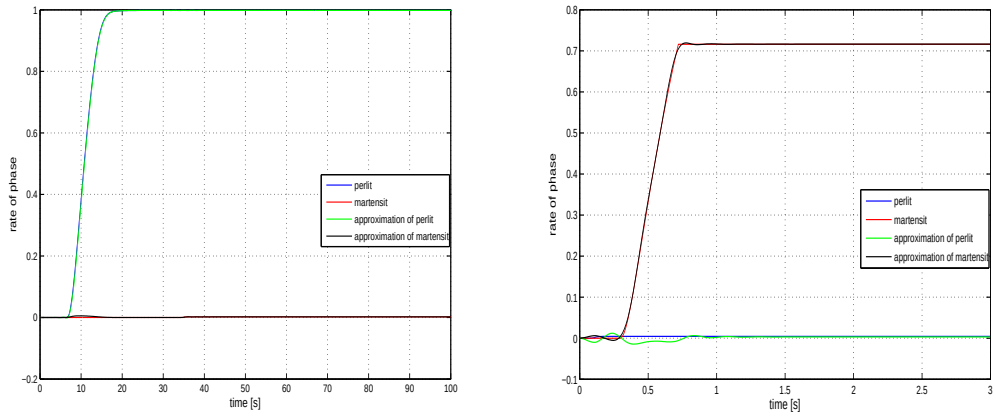


FIGURE 5. Results of the identification process for slow (left) and fast (right) quenching.

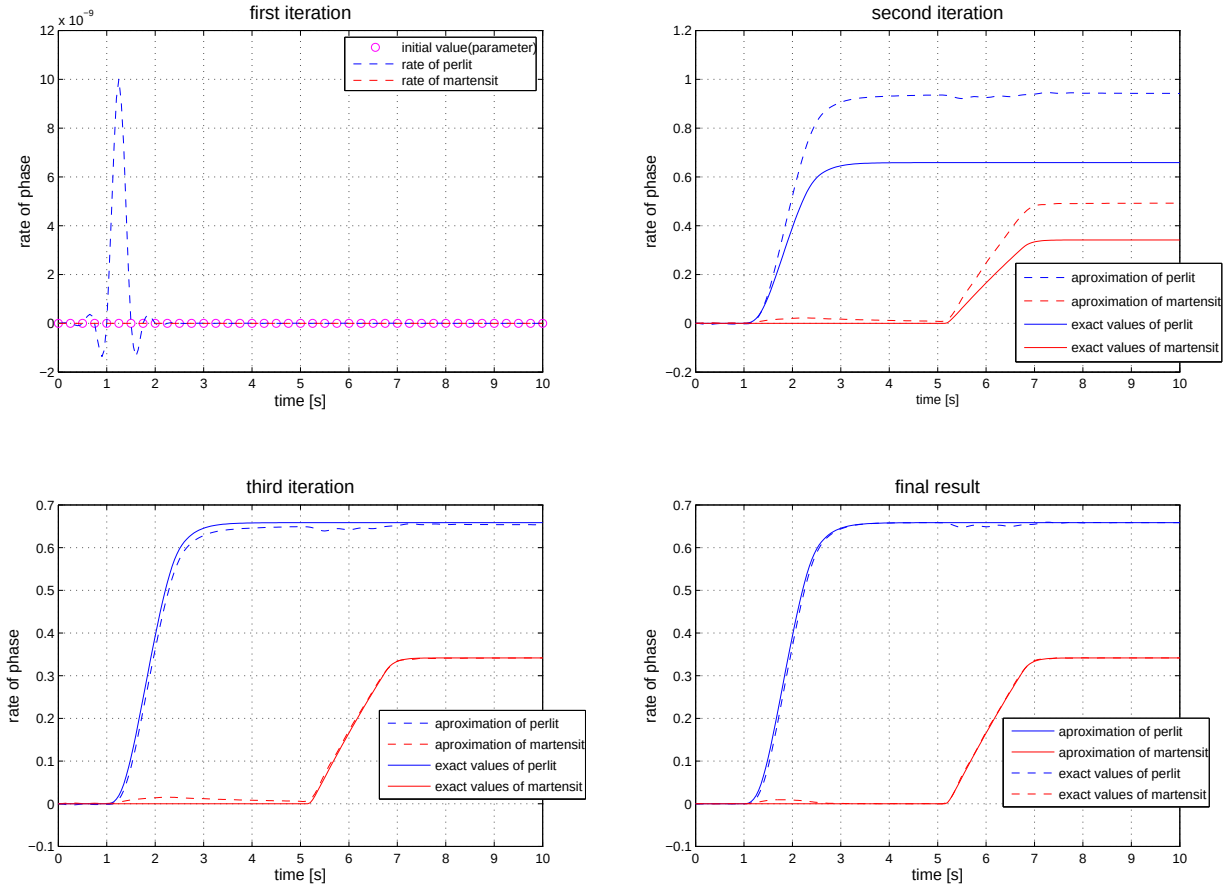


FIGURE 6. Three iterations and final resulting phase fraction curves in the case of moderate cooling.

martensite ($z$) only grows, as long as a certain temperature dependent threshold value is not exceeded.

Figure 4 shows the resulting model dilatometer curves for the case of slow, moderate and fast cooling, respectively. Especially the case of moderate cooling (see also Figure 2) is of interest, since it exhibits two phase transitions. Based on this model data, we have used the MATLAB Levenberg-Marquardt routine to solve the discretized optimization problem (4.1). To obtain useful results an equilibrating of both terms in the cost functional is indispensable. To this end we have defined

$$\omega_1 = 10^4, \qquad \omega_2 = \frac{1}{(\hat{\tau}(0) - \hat{\tau}(T))^2}.$$

Figure 5 shows the results of the identification in the case of fast and slow cooling in comparison with the exact result. We can conclude that indeed the identification was successful. However, the really interesting case is the one with moderate cooling, which exhibits two phase transitions. Figure 6 shows three iterations and the final result of the optimization process in this case. Starting from initial values $y_0 = z_0 \equiv 0$, already after three iterations the correct final phase fraction has ben reached. This is particularly important since as described in the introduction, the standard way of obtaining the resulting phase fraction values in the case of several phase transitions requires expensive and time-consuming optical measurements.

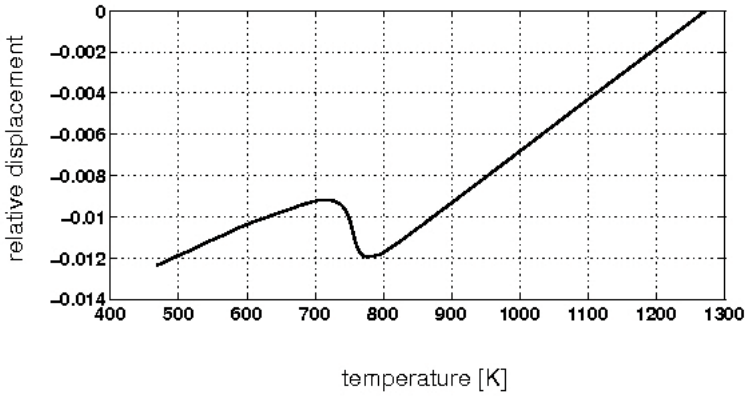


FIGURE 7. Model dilatometer curve perturbed with white noise.

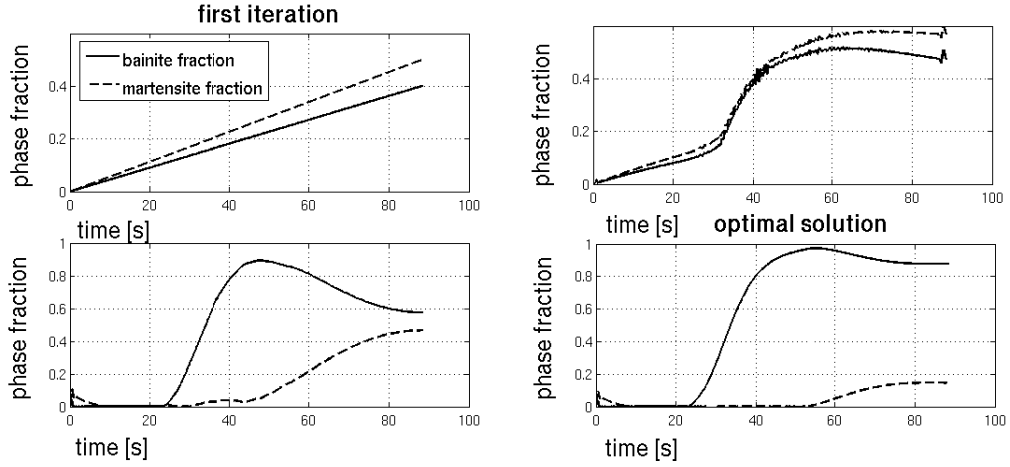


FIGURE 8. Model dilatometer curve perturbed with white noise.

Figure 7 depicts a measured dilatometer curve for the steel 16MnCr5. One phase transition between $730K$ and $780K$ (from austenite to bainite) can easily

be seen, another one between $580K$ and $620K$ (from austenite to martensite) is hardly visible. However, our numerical method indeed is able to detect both phase transitions. Figure 8 shows four iterations for this case. From physical point of view one would expect a monotone behaviour of the phase fraction curve, which holds only true for one of them. However, the final phase fractions for both phases correspond to the measured ones with a relative error of less than 10%. Further details can be found in [6]

## References


[1] D. Hömberg, A. Khludnev, *A thermoelastic contact problem with a phase transition*, IMA J. Appl. Math., 71 (2006), 479–495.

[2] D. Hömberg, W. Weiss, *PID control of laser surface hardening of steel*, IEEE Trans. Control Syst. Technol., 14 (2006), 896–904.

[3] D. Hömberg, M. Yamamoto, *On an inverse problem related to laser material treatments*, Inverse Problems, 22 (2006), 1855–1867.

[4] S. Jiang, R. Racke, *Evolution equations in thermoelasticity*, Chapman & Hall/CRC, Boca Raton, 2000.

[5] A. I. Prilepko, D. G. Orlovsky, I. A. Vasin, *Methods for Solving Inverse Problems in Mathematical Physics*, Marcel Dekker, New York, 2000.

[6] P. Suwanpinij, N. Togobytska, C. Keul, W. Weiss, U. Prahl, D. Hömberg, W. Bleck, *Phase transformation modeling and parameter identification from dilatometric investigations*, WIAS Preprint No. 1306 (2008), to appear in Steel Res.

[7] Tanabe, H., *Equations of Evolution*. Pitman, London, 1979.